Umm Al-Qura Univ. J. Eng.& Arch. Vol. 1, No.1, pp. 83-94 (2009) *29-01-004 © The University Press*

Influence of Whirl on Design, Operation and Performance Parameters at Nozzles Exit of an Axial Gas Turbine Stage

Saleh A. Akeel

صالح علوي عقيل

Mechanical Engineering Department, Umm Al-Qura University, Makkah, Saudi Arabia.

تأثير التدويم على معامِلات التصميم والتشغيل والأداء بمخرج فوهة لتربينة محورية غازية ذات مرحلة

أظهرت الدراسة الحالية أن هناك تأثيرا كبيرا للتدويم على معظم المعامِلات. عند القمة، نقصت زاوية السرعة النسبية بـ ١٠٠٪ للدوامات الحرة من قيمتها عند القاع و ٩١,٢٪ للدوامات القسرية. ونقصت سرعة التدويم والسرعة النسبية بـ ٢٥,١٪ & ٢٣٪، على التوالي للدوامات الحرة و ١٨,٩٪ & ٣٢,٥٪ للدوامات القسرية. عند مخرج الفوهة وفي الظروف نفسها، كانت درجة الحرارة للغاز المثالي أعلى منها للهواء المثالي بـ ١,٣٦-٢,٢٪، وللسريان الفعلي أعلى منه للمثالي بـ ٠,٥٣-٠,٨٤٪ نتيجة للاحتكاك. وكان ضغط الغاز للسريان الفعلي أعلى منه للمثالي بـ ١,٩٦-٣,١٧٪ وللدوامات القسرية أعلى منه للدوامات الحرة بـ ٠,٢٨-٠,٥٦٪ وللغاز أعلى منه للهواء بـ ٠,١٩-٠,٥٢٪. وكانت الكثافة للسريان الفعلي أعلى منها للمثالي بـ ١,٤٢-٢,٣٢٪ وللهواء أعلى منها للغاز بـ ١,١٥-١,٦٤٪. إن درجة الحرارة والضغط والكثافة ازدادت مع نصف القطر بـ ٥,٦٪، ٢٢,٥٪ و ١٦٪، على التوالي من قيمها عند القاع. كان الماخ النسبي للغاز أعلى منه للهواء بـ ١,٣٨-١,٧٩٪، وللسريان المثالي أعلى منه للفعلي بـ ٠,٢٦-٠,٤٢٪. وكان الماخ للدوامات القسرية أعلى منه للدوامات الحرة بـ ٣,٦٣٪ عند القاع بينما كان أقل منه بـ ٩,٢٪ عند القمة. نقص الماخ للدوامات الحرة مع نصف القطر بـ ٣١,٢٪ و ٣٠,٧٪ من قيمته عند نصف القطر المتوسط للهواء والغاز على التوالي و ٤٤,٢ و ٤٣,٧٪ للدوامات القسرية. إن كل القيم المحسوبة للماخ عند القاع، ٠,٥٧٧-٠,٦٠٦، كانت أقل من أعلى قيمة موصى بها، ٠,٧٥.

Abstract

The present study shows that the whirl has a considerable effect on most parameters. At the tip, the normalized relative velocity angle decreased by 100% of its value at the root for free-vortex and 91.2% for forced-vortex. Also, the normalized whirl and relative velocities decreased by 25.1% & 23%, respectively for free-vortex flow and 18.9% & 32.5% for forced-vortex. For the same conditions, the normalized temperature of ideal gas was higher than that of ideal air by 1.36-2.2% and of actual flow was higher than of ideal flow by 0.٥٣-0.٨٤% due to friction. In addition, the normalized pressure of actual flow was higher than that of ideal flow by 1.96-3.17%, of forced-vortex was higher than of free-vortex by 0.28-0.56% and of ideal gas was higher than of ideal air by 0.19-0.52%. Moreover, the normalized density of actual flow was higher than that of ideal flow by 1.42-2.32% and of ideal air was higher than of ideal gas by 1.15-1.64%. The normalized temperature, pressure and density increased over the radius by 5.6%, 22.5% and 16%, respectively. Further, the relative Mach number of ideal gas was higher than that of ideal air by 1.38-1.79% and of ideal flow than of actual flow by 0.26-0.42%. At the root, such Mach of forced-vortex was higher than that of free-vortex by 3.63% while it was lower by 9.2% at the tip. Such Mach for free-vortex decreased by 31.2% and 30.7% over the radius for ideal air and ideal gas, respectively while for forced-vortex flow the decrease were 44.2% and 43.7%. All computed Mach number values at the root, 0.577-0.606, were less than the upper recommended, 0.75.

Keywords: Axial gas turbine stage, free/forced-vortex positive whirl, different parameters.

INTRODUCTION

Free and forced vortex whirl of ideal and actual flows of ideal air and ideal gas were used to compute the operating parameters at nozzle blades exit of an axial gas turbine stage. The radial changes were ignored in the annulus of an axial gas turbine stage. Thus, such assumption is reasonable for short blades with root to tip radius ratio greater than 0.8. This is typical in front stages of a gas turbine (Cohen et al. 2001; Logan 1993; Yahya 1983). The last stages have low radius ratio of 0.4 (Mattingly 1996) to pass high mass flux in a small overall diameter engines. The taper of the annulus causes the streamline surfaces of revolution not to be parallel to the rotor axis. Hence, the actual flow has a very small radial velocity component compared with the axial and whirl components (Cohen et al. 2001).

The flow at nozzle blades exit is given a positive whirl velocity in impeller direction of rotation. This whirl flow results are due to nozzle blades angle at exit. Thus, the static temperature and static pressure change with the radius. Thereby, the flow experiences a small radial changes. With low radius ratio blades, the peripheral speed changes much between the root and tip. Hence, the velocity diagrams and the resulting gas angles vary too. The change of such temperature and pressure vary the density and, in turn, the magnitudes of velocity vectors change. Therefore, a further change of velocity triangles occurs (Kerrebrock 1992; Yahya 1983). As a result, the gas angles at the mean radius become far from those at the root or tip of the blade row, but the elements of gas between blade rows are in radial equilibrium (Cohen et al. 2001). For high efficiency operation, the gas angles must approximately match the blade angles at all radii. This results in a twisted vortex balding (Cohen et al. 2001).

Computation of mass flow rate through an axial gas turbine stage was done by different methods using free-vortex flow (Najjar & Akeel 2007). The parabolic density profile from root to tip of such study gave the most accurate mass flow rate. The absolute velocity angle and axial velocity were constants along the nozzle blades exit for forced-vortex and for free-vortex flows, respectively (Cohen et al. 2001; Dixon 2006). The velocity triangles at the nozzle blades exit of the actual flow were not much affected by friction in such nozzles (Cohen et al. 2001). The upper recommended value of the relative Mach number at the root should not exceed 0.75 in an axial gas turbine stage (Cohen et al. 2001). Calculations of performance and design parameters in turbomachinery were done using radial equilibrium and streamline curvature methods (Macchi 1984; Smith 1966).

The present objective is to investigate the effect of free-vortex and forced-vortex positive whirl of actual and ideal flows using ideal air and ideal gas on the design, operation and performance parameters at nozzle blades exit of an axial gas turbine stage.

THEORETICAL ANALYSIS

In the present study, the equations for design, operation and performance parameters besides their solutions are at convergent nozzle blades exit of an axial gas turbine stage. The flow from nozzles exit enters the rotor, which generates the power. To compute this power, the specific work from the rotor should be calculated at a convenient radius and multiplied by the correct mass flow rate (Najjar & Akeel 2007). The correct flow rate is an important parameter for design, operation and performance of gas turbine. Introducing a positive whirl velocity, C_{w2}, at nozzle blades exit changes the static pressure, P_2, and static temperature, T_2, there. Hence, P_2 and absolute velocity, C_2, vary from root to tip, see Fig. 1. Thus, the density, ρ_2, changes there too.

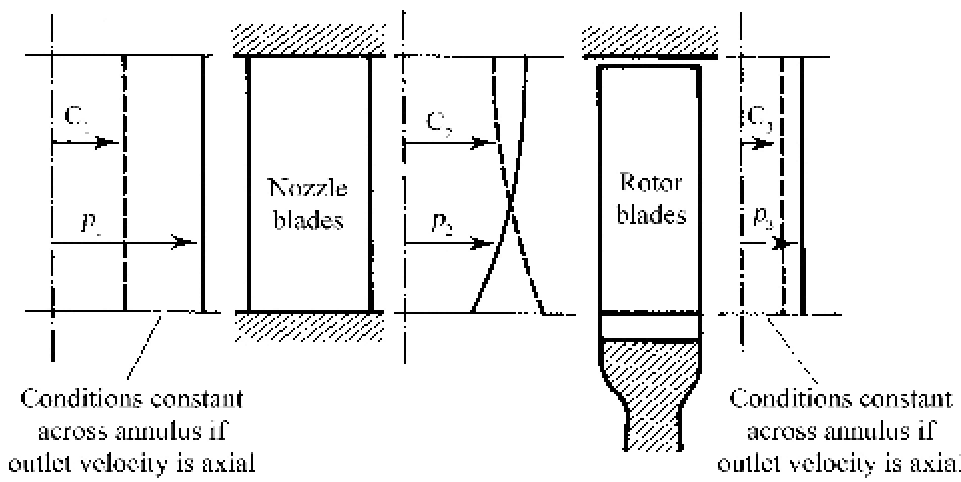

Fig. 1: Variation of P_2 and C_2 across the annulus of a turbine stage with free-vortex-flow.

Forced-vortex flow has constant absolute velocity angle, $\alpha_2 = \alpha_{2m}$ = constant, along nozzle blades exit and the axial velocity, C_{a2}, there is given by (Cohen et al. 2001; Dixon 2006)

$$C_{a2} = C_{a2m}\left(\frac{r_{2m}}{r_2}\right)^{\sin^2(\alpha_{2m})} \quad (1)$$

where, α_{2m} is α_2 at the mean radius, $r_{2m} = (r_{2r} + r_{2t})/2$, C_{a2m} is C_{a2} at r_{2m}, r_2 is the radius, r_{2r} and r_{2t} are the root and tip radii, respectively. In free-vortex whirl flow $C_{a2} = C_{a2m}$ at r_2 and α_2 is given by (Cohen et al. 2001; Dixon 2006)

$$\alpha_2 = \tan^{-1}\left\{\left(\frac{r_{2m}}{r_2}\right)\tan(\alpha_{2m})\right\} \quad (2)$$

In both free-vortex and forced-vortex positive whirl flows, the relative velocity angle, β_2, is related to α_{2m} by (Dixon 2006; Sayers 1990)

$$\beta_2 = \tan^{-1}\left\{\left(\frac{r_{2m}}{r_2}\right)\tan\left(\alpha_{2m}\right) - \left(\frac{r_2}{r_{2m}}\right)\left(\frac{U_{2m}}{C_{a2}}\right)\right\} \tag{3}$$

where, $U_{2m} = \omega\, r_{2m}$ is the peripheral speed at r_{2m} and ω is the angular velocity. The relative velocity, V_2, C_{w2} and C_2 may be found using Fig. 2. Thus, we have

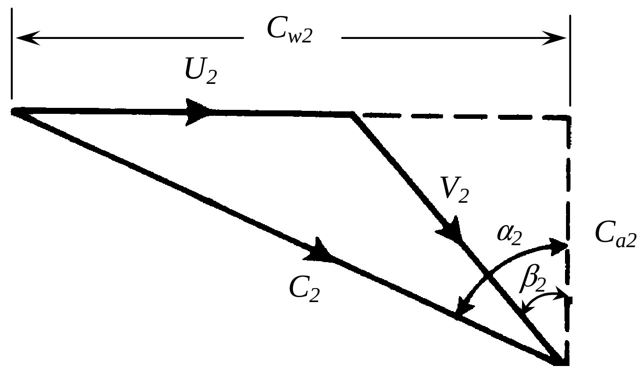

Fig. 2: Velocity triangle for a particular r_2 at nozzle blades exit.

$$C_{w2} = C_{a2}\tan(\alpha_2) \tag{4}$$

$$C_2 = \frac{C_{a2}}{\cos(\alpha_2)} \tag{5}$$

$$V_2 = \frac{C_{a2}}{\cos(\beta_2)} \tag{6}$$

Since there is no work done in nozzles thus, $T_{01} = T_{02}$ where, T_{01} and T_{02} are the stagnation temperatures at inlet and exit of nozzle blades, respectively. For ideal flow using ideal air or ideal gas, the operation parameters T_{2I}, P_{2I}, ρ_{2I} and performance one (relative Mach number, M_{2I}) for free-vortex or forced-vortex positive whirl flows are given by

$$\frac{T_{2I}}{T_{02}} = 1 - \frac{C_2^2}{2C_P T_{02}} \tag{7}$$

$$\frac{P_{2I}}{P_{02}} = \left(\frac{T_{2I}}{T_{02}}\right)^{\frac{\gamma}{\gamma-1}} \tag{8}$$

$$\frac{\rho_{2I}}{\rho_{02}} = \frac{P_{2I}}{P_{02}} \Big/ \frac{T_{2I}}{T_{02}} \tag{9}$$

and

$$M_{2I} = \frac{V_2}{\sqrt{\gamma R_0 T_{2I}}} \tag{10}$$

where, the subscript I denotes the ideal flow, C_p is the mean specific heat at constant pressure, P_{02} is the stagnation pressure, γ is the specific heats ratio, ρ_{02} is the stagnation density and R_0 is the ideal gas constant. For actual flow, it is assumed that the velocity triangles are negligibly affected by friction in nozzle blades (Cohen et al. 2001). Thus, T_{2A}, P_{2A}, ρ_{2A} and M_{2A} are affected and for free-vortex or forced-vortex positive whirl using ideal air or ideal gas. They are

$$\frac{T_{2A}}{T_{02}} = \lambda_n + (1-\lambda_n)\frac{T_{2I}}{T_{02}} \tag{11}$$

$$\frac{P_{2A}}{P_{02}} = \left(\frac{T_{2A}}{T_{02}}\right)^{\frac{\gamma}{\gamma-1}} \tag{12}$$

$$\frac{\rho_{2A}}{\rho_{02}} = \frac{P_{2A}}{P_{02}} \Big/ \frac{T_{2A}}{T_{02}} \tag{13}$$

and

$$M_{2A} = \frac{V_2}{\sqrt{\gamma R_0 T_{2A}}} \tag{14}$$

where, the subscript A denotes the actual flow and λ_n is the nozzle loss coefficient.

COMPUTATION PROCEDURE

Calculations were done for free-vortex and forced-vortex positive whirl actual flow (λ_n = 5%) and ideal flow of ideal air (γ = 1.4) and ideal gas (γ = 1.333) at nozzle blades exit of an axial gas turbine stage (Cohen et al. 2001).

Solution of Eqs. (2) to (6) gives the design (α_2, β_2) and operating parameters (C_{w2}, C_2 and V_2) using free-vortex positive whirl flow. As well, solution of Eqs. (1) and (3) to (6) produces the same parameters with the operating parameter C_{a2} replaces the design parameter α_2 for forced-vortex positive whirl flow. The variation of such parameters with the radius depends only on introduced free-vortex or forced-vortex positive whirl flow. In addition, solution of Eqs. (7) to (14) gives the other operating parameters (T_{2I}, P_{2I}, ρ_{2I}) as well as the performance parameter M_{2I} for ideal flow and (T_{2A}, P_{2A}, ρ_{2A} and M_{2A}) for actual flow using free-vortex and forced-vortex positive whirl of ideal air and ideal gas. Design, operation and performance parameters were computed at nozzle blades exit from r_{2r} to r_{2t} of an axial gas turbine stage.

The computed parameters were normalized except for M_2, which is already dimensionless. The normalized parameters are $\alpha_{2n} = \alpha_2/\beta_{2m}$, $\beta_{2n} = \beta_2/\beta_{2m}$, $C_{a2n} = C_{a2}/C_{a2m}$, $C_{2n} = C_2/C_{a2m}$, $C_{w2n} = C_{w2}/C_{a2m}$, $V_{2n} = V_2/C_{a2m}$, $T_{2n} = T_2/T_{02}$, $P_{2n} = P_2/P_{02}$ and $\rho_{2n} = \rho_2/\rho_{02}$. Such normalized parameters and M_2 vary with the normalized r_2, $r_n = r_2/r_{2r}$, from r_{2r} to r_{2t}. Thus, the present results become more general and applicable for other geometries and operating conditions.

The particulars required for the present computations were chosen for an axial gas turbine stage used in a business aircraft engine (Cohen et al. 2001). Such data are r_{2r} = 0.185 m, r_{2t} = 0.247 m, α_{2m} = 58.383°, β_{2m} = 20°, N = 250 rps, C_{a2m} = 272 m/s, T_{02} = 1100 K, λ_n = 0.05, $(C_p)_G$ = 1.148 kJ/(kg.K) and $(\gamma)_G$ = 1.333. These data were also documented (Bathie 1996; Logan 1993; Wilson & Korakianitis 1998).

RESULTS AND DISCUSSION

At nozzle blades exit, Fig. 3 shows the variation of the design parameters α_{2n} and β_{2n} besides the operating ones C_{2n}, C_{a2n}, V_{2n} and C_{w2n} with r_n. These parameters decrease gradually with r_n from root to tip. α_{2n} of forced-vortex and C_{a2n} of free-vortex flows are constant over r_n thus, they are not presented. At the tip, α_{2n} of free-vortex flow decreased with r_n by 12.1% based on its value at r_{2r}. The rate of decrease of α_{2n} with r_n was much lower than that for β_{2n} besides α_{2n} was always bigger than β_{2n} over r_n. The rate of decrease of β_{2n} with r_n for free-vortex flow was higher than that for forced-vortex. β_{2n} of free-vortex was bigger than that for forced-vortex at the root and the opposite was true at the tip. Also, β_{2n} decreased with r_n by 100% for free-vortex flow and 91.2% for forced-vortex. Thus, V_2 was axial at the tip for free-vortex flow while it was 8.8% far from axial there for forced-vortex. In addition, C_{2n} of forced-vortex and free-vortex flows almost coincide and each decreased with r_n by 19%. C_{2n} was always bigger than the other velocities over r_n. The rate of decrease of C_{w2n} for free-vortex was higher than that for forced-vortex flow. C_{w2n} for free-vortex was bigger than that for forced-vortex at the root and the opposite was true at the tip. Moreover, C_{w2n} decreased with r_n by 25.1% for free-vortex and 18.9% for forced-vortex flow. Further, V_{2n} decreased with r_n by 23% for free-vortex and 32.5% for forced-vortex. V_{2n} of free-vortex flow was bigger than V_{2n} of forced-vortex at the root and the opposite was true at the tip. Furthermore, C_{a2n} for forced-vortex flow decreased with r_n by 18.9% while its value was 1 at r_{2m} thus, C_{a2} equals to C_{a2m}.

At nozzle blades exit, Fig. 4 shows that the operating parameter T_{2n} increases gradually with r_n from root to tip. For the same conditions, T_{2n} values of ideal gas were higher than those of ideal air by an average of 2.2% based on the value of ideal air at the root and 1.36% at the tip. Further, T_{2n} values of actual flow were higher than those of ideal flow by an average of 0.84% based on the value of ideal flow at the root and 0.53% at the tip due to friction in nozzle blades. The difference in T_{2n} decreased in the first case and slightly decreased in the second with r_n. In addition, T_{2n} values of forced-vortex flow were higher than those of free-vortex by an average of 0.16 % based on the value of free-vortex at the root and 0.09% at the tip. In this case, the difference in T_{2n} slightly decreased as r_n increases up to zero at r_{2m} then slightly increased. Moreover, T_{2n} increased by an average of to 5.6%

based on the value at the root over r_n. Thus, the major effect on T_{2n} was due to r_n variation and the second was if ideal gas replaces ideal air while such effect was small if actual flow replaces ideal flow and was negligible if forced-vortex replaces free-vortex flow.

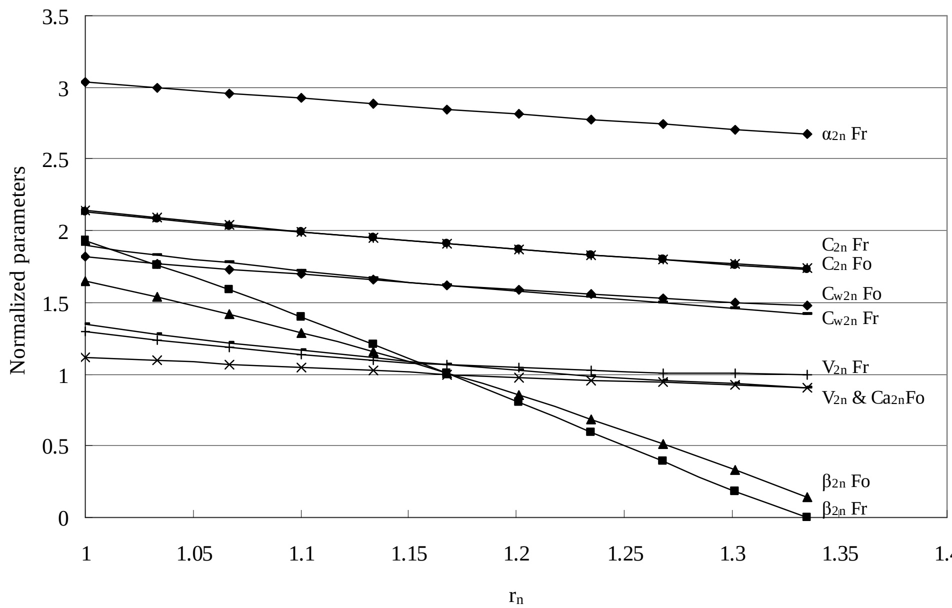

Fig. 3: Variation of several normalized parameters with r_n at nozzle blades exit.

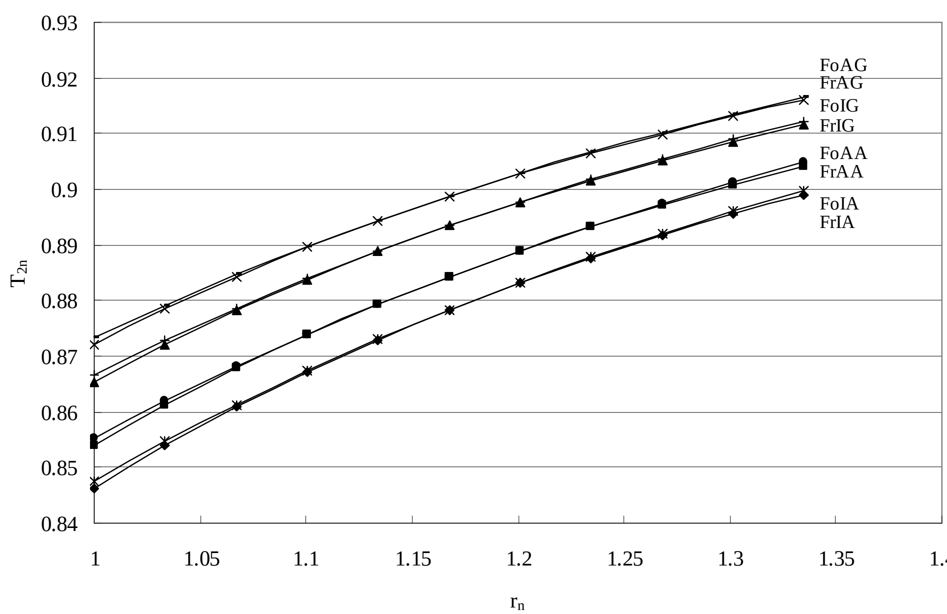

Fig. 4: Variation of T_{2n} with r_n at nozzle blades exit.

At nozzle blades exit, Fig. 5 indicates that the operating parameter P_{2n} increases gradually with r_n from root to tip. For the same conditions, P_{2n} values of actual flow were higher than those of ideal flow by an average of 3.17% based on ideal flow value at the root and 1.96% at the tip. Besides, P_{2n} values of ideal gas were higher than those of ideal air by an average of 0.52% based on ideal air value at the root and 0.19% at the tip. The difference in P_{2n} decreased in the first case and slightly decreased in the second with r_n. In addition, P_{2n} values of forced-vortex flow were higher than those of free-vortex by an average of 0.56% based on free-vortex flow value at the root and 0.28% at the tip. The difference in P_{2n} of this case slightly decreased with r_n to zero at r_{2m} then slightly increased. Moreover, P_{2n} increased by an average of 22.5% based on the value at root over r_n. Thus, the major effect on P_{2n} was due to r_n variation and the second was if actual flow replaces ideal flow while the effect if forced-vortex flow replaces free-vortex and ideal gas replaces ideal air was small.

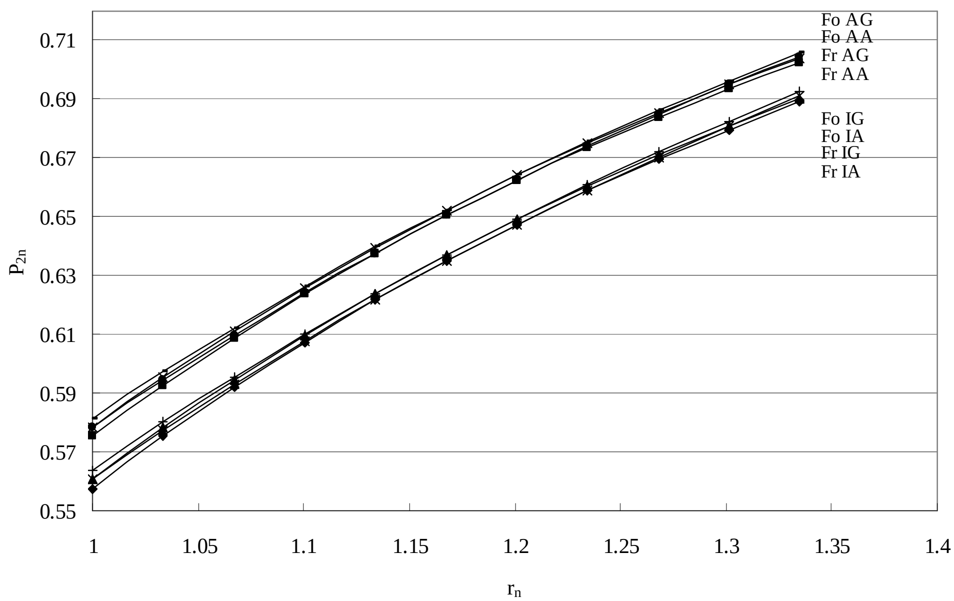

Fig. 5: Variation of P_{2n} with r_n at nozzle blades exit.

At nozzle blades exit, Fig. 6 reflects that the operating parameter ρ_{2n} increases gradually with r_n from root to tip. For the same conditions, ρ_{2n} values of actual flow were higher than those of ideal flow by an average of 2.32% based on ideal flow value at the root and 1.42% at the tip. Also, ρ_{2n} values of ideal air were higher than those of ideal gas by an average of 1.64% based on ideal air value at the root and 1.15% at the tip. The difference in ρ_{2n} decreased in the first case and slightly decreased in the second with r_n. In addition, ρ_{2n} values of forced-vortex flow were higher than those of free-vortex by an average of 0.41% based on free-vortex flow value at the root and 0.2 at the tip. In this case, the difference in ρ_{2n} slightly decreased as r_n increases up to zero at r_{2m} then slightly increased. Moreover, ρ_{2n} increased with r_n by an average of 16% based on the value at root over r_n. Thus, the major effect on ρ_{2n} was due to r_n variation, the second was if actual flow replaces ideal flow and the third was if ideal air replaces ideal gas while if forced-vortex flow replaces free-vortex the effect was small.

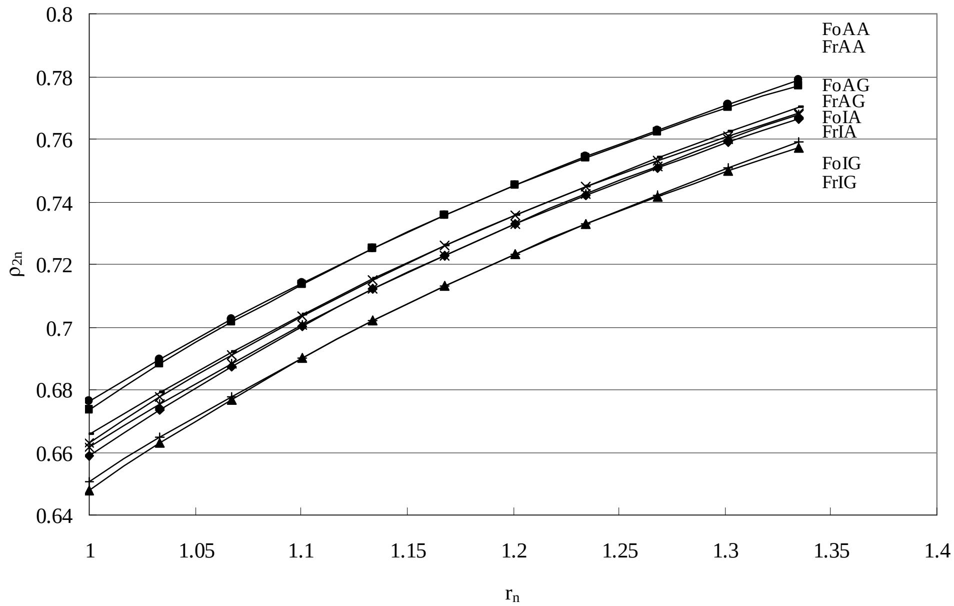

Fig. 6: Variation of ρ_{2n} with r_n at nozzle blades exit.

At nozzle blades exit, Fig. 7 shows that the main important performance parameter M_2 decreases gradually with r_n from root to tip. For the same conditions, M_2 values of ideal gas were higher than those of ideal air by an average of 1.38% based on the value of ideal air at the root, 1.64% at r_{2m} and 1.79% at the tip. In this case, the difference in M_2 increased with r_n. As well, M_2 values of ideal flow were higher than those of actual flow by an average of 0.42% based on the value of ideal flow at the root and 0.26% at the tip. In this case, the difference in M_2 decreased with r_n. In addition and at the root, M_2 values of forced-vortex flow were higher than those of free-vortex flow by 3.63% based on the value of free-vortex. Moreover and at the tip, M_2 values of free-vortex flow were higher than those of forced-vortex flow by 9.2% based on the value of free-vortex. At r_{2m}, M_2 values of free-vortex flow were exactly the same as those of forced-vortex for ideal gas and the same was true for ideal air but with a lower value. Further, M_2 values for free-vortex decreased by 31.2% and 30.7% based on the value at r_{2m} over r_n for ideal air and ideal gas, respectively while for forced-vortex flow the decrease were 44.2% and 43.7%. In this case, the difference in M_2 decreased with r_n up to zero at r_m for each of the ideal gas and ideal air then increased. Thus, the major effect on M_2 was due to r_n variation, the second was if forced-vortex replaces free-vortex and the third was if ideal gas replaces ideal air, while if ideal flow replaces actual flow the effect was small. All the computed M_2 values at the root, 0.577-0.606, were less than the upper recommended, 0.75.

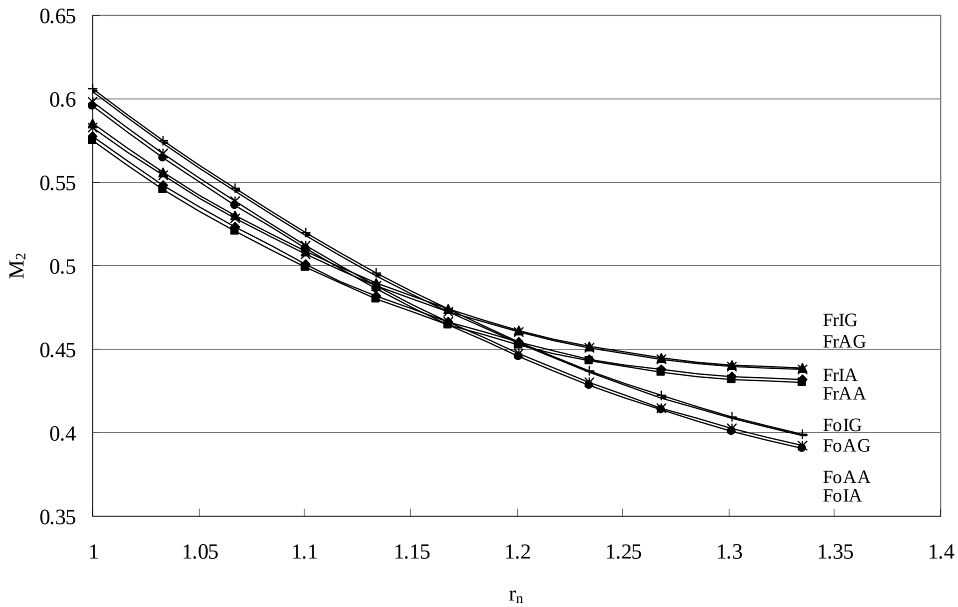

Fig. 7: Variation of M_2 with r_n at nozzle blades exit.

CONCLUSIONS

The present study reflected that there is a remarkable effect of whirl on most parameters. At the tip, the normalized relative velocity angle decreased by 100% of its value at the root; for free-vortex thus, it was axial; and 91.2% for forced-vortex thereby, it was 8.8% far from axial. In addition, the normalized positive whirl and relative velocities decreased by 25.1% and 23%, respectively for free-vortex whirl flow besides 18.9% and 32.5% for forced-vortex.

For the same conditions, the normalized temperature of ideal gas was higher than that of ideal air by 1.36-2.2% and of actual flow was higher than that of ideal flow by 0.53-0.84% due to friction. Besides that, the normalized pressure of actual flow was higher than that of ideal flow by 1.96-3.17%, of forced-vortex was higher than of free-vortex by 0.28-0.56% and of ideal gas was higher than that of ideal air by 0.19-0.52%. In addition, the normalized density of actual flow was higher than that of ideal flow by 1.42-2.32% and of ideal air was higher than that of ideal gas by 1.15-1.64%. The normalized temperature, pressure and density increased with the normalized radius by 5.6%, 22.5% and 16%, respectively. Moreover, the relative Mach number of ideal gas was higher than that of ideal air by 1.38-1.79% and of ideal flow was higher than that of actual flow by 0.26-0.42%. At the root and the same conditions, such Mach of forced-vortex was higher than that of free-vortex by 3.63% while it was lower by 9.2% at the tip. At the mean radius, the Mach number value of free-vortex was exactly the same as that of forced-vortex for ideal gas and the same was true for ideal air with the ideal gas value was higher than that of ideal air. Such Mach values for free-vortex decreased by 31.2% and 30.7% over the normalized radius for ideal air and ideal gas, respectively, while the decrease was 44.2% and 43.7% for forced-vortex flow. All computed Mach values at the root, 0.577-0.606, were less than the upper recommended, 0.75.

NOMENCLATURE

C_2 : absolute velocity, m/s
C_{2n} : normalized C_2, C_2/C_{a2m}
C_{a2} : axial velocity, m/s
C_{a2n} : normalized C_{a2}, C_{a2}/C_{a2m}
C_{a2m} : C_{a2} at r_{2m}, m/s
C_P : mean specific heat at constant pressure, kJ/(kg.K)
C_{w2} : positive whirl velocity, m/s
C_{w2n} : normalized C_{w2}, C_{w2}/C_{a2m}
M_2 : relative Mach number
N : rotor rotational speed, rps
P_{02} : stagnation pressure, kPa
P_2 : static pressure, kPa
P_{2n} : normalized P_2, P_2/P_{02}
R_0 : ideal gas constant, kJ/(kg.K)
r_n : normalized r_2, r_2/r_{2r}
r_2 : radius, m
r_{2m} : mean radius, $(r_{2t} + r_{2r})/2$, m
r_{2r} : root radius, m
r_{2t} : tip radius, m
T_{02} : stagnation temperature, K
T_2 : static temperature, K
T_{2n} : normalized T_2, T_2/T_{02}
U_{2m} : peripheral speed at r_{2m}, m/s
V_2 : relative velocity, m/s
V_{2n} : normalized V_2, V_2/C_{a2m}

GREEK SYMBOLS

α_2 : absolute velocity angle, degrees
α_{2n} : normalized α_2, α_2/β_{2m}
α_{2m} : α_2 at r_{2m}, degrees
β_2 : relative velocity angle, degrees
β_{2n} : normalized β_2, β_2/β_{2m}
β_{2m} : β_2 at r_{2m}, degrees
γ : specific heat ratio
λ_n : nozzle loss coefficient, $(T_{2A} - T_{2I})/(T_{02} - T_{2I})$
ρ_{02} : stagnation density, kg/m^3
ρ_2 : density, kg/m^3
ρ_{2n} : normalized ρ_2, ρ_2/ρ_{02}
ω : angular velocity, s^{-1}

SUBSCRIPTS

1,2,3 : at nozzle blades inlet, exit and at rotor exit

A : actual flow
G : ideal gas
I : ideal flow

ABBREVIATIONS

Fr : free-vortex flow
FrAA : free-vortex actual flow of ideal air
FrAG : free-vortex actual flow of ideal gas
FrIA : free-vortex ideal flow of ideal air
FrIG : free-vortex ideal flow of ideal gas
Fo : forced-vortex flow
FoAA : forced-vortex actual flow of ideal air
FoAG : forced-vortex actual flow of ideal gas
FoIA : forced-vortex ideal flow of ideal air
FoIG : forced-vortex ideal flow of ideal gas

REFERENCES

Bathie, W. W. 1996. *Fundamentals of Gas Turbines*. John Wiley and Sons, New York, 2nd ed.

Cohen, H. Rogers, G. F. C. & Saravanamuttoo, H. I. H. 2001. *Gas Turbine Theory*. Longman, London, 5th ed.

Dixon, S. L. 2006. *Fluid Mechanics and Thermodynamics of Tturbomachinery*. Butterworth-Heiman, UK, 5th ed.

Kerrebrock, J. L. 1992. *Aircraft Engines and Gas Turbines*. MIT press, Cambridge, Massachusetts, 2nd ed.

Logan, E. 1993. *Turbomachinery: Basic theory and applications*. Marcel Dekker, New York, 2nd ed.

Macchi, E. 1984. "The use of radial equilibrium and streamline curvature methods for turbomachinery design predictions". Int. *Thermodynamics and Fluid Machines of Turbomachinery*, Martines Nighoff, 1: 133-166.

Mattingly, J. D. 1996. *Elements of Gas Turbine Propulsion*. McGraw-Hill, New York.

Najjar, Y. S. & Akeel, S. A. M. S. 2007. "Evaluation of mass flow through an axial gas turbine stage using different computational methods", *Journal of Process Mechanical Engineering*, Professional Engineering Publishing Ltd. (Accepted)

Sayers, A. T. 1990. *Hydraulic and Compressible Flow Turbomachines*. McGraw-Hill, London. Smith, L. H. Jr. 1966. The radial equilibrium equation of turbomachinery. Trans. ASME, Series A, 88:.

Wilson, D. G. & Korakianitis, T. 199**8**. *The Design of High Efficiency Turbomachinery and Gas Turbines*. Prentice Hall, New Jersey, 2nd ed.

Yahya, S. M. 1983. *Turbines, Compressors and Fans*. Tata McGraw-Hill, New Delhi.

Received 25/1/1429; 3/2/2008, accepted 26 /11/1429; 24/11/2008